PULSED-DISCHARGE CARBON DIOXIDE LASERS

David V. Willetts
Royal Signals and Radar Establishment
Great Malvern, Worcs, UK

INTRODUCTION

The purpose of this review is to attempt a general introduction to pulsed carbon dioxide lasers of the kind used or proposed for laser radar applications. There is a strong bias towards understanding those features of operation which impact strongly on gas lifetime issues, and so a decision has been made to omit mention of the theory of laser beams and resonators and the diffraction optics used to describe them. Nevertheless, laser physics is an excellent example of a cross-disciplinary topic, and the molecular spectroscopy, energy transfer, and plasma kinetics of the devices will be explored.

The review is structured to begin by introducing the concept of stimulated emission and population inversions, leading on to the molecular spectroscopy of the CO_2 molecule. This is followed by a consideration of electron-impact pumping, and the pertinent energy transfer and relaxation processes which go on. Since the devices are plasma pumped it is necessary to introduce a complex subject, but this is restricted to appropriate physics of glow discharges. Examples of representative devices are shown, and the review concludes with the implications of the foregoing to plasma chemistry and gas life.

STIMULATED EMISSION (Ref. 1)

Consider the two-level system shown in figure 1. Radiation of frequency E/h causes upward transitions from level 1 to level 2 at a rate $B_{12}IN_1$ where I is the intensity of illumination. Spontaneous emission or collisions cause a dissipative loss from level 2 at a rate $A_{21}N_2$. The nett effect of these processes is the well-known phenomenon of absorption of the incident radiation. However, there is a further process of stimulated emission, akin to (stimulated) absorption, which proceeds at a rate $B_{21}N_2I$. This is not observed with light of low intensity in thermal equilibrium, because the upper state population $(B_{12}/A_{21})N_1I$ is exceedingly low under such conditions. However if we can depart dramatically from thermal equilibrium and set up a condition where $N_2 > N_1$ (a so-called population inversion), the emissive rate $B_{21}IN_2$ exceeds absorption and the latter is replaced by gain, a condition of negative absorption. This arises because it is possible to show by quantum theory that $B_{12} = B_{21} = B$, so that

$$\frac{dI}{dt} = c\frac{dI}{dx} \quad \alpha\left[N_2 - N_1\right]BI \qquad (1)$$

(which reduces to the familiar Beer's Law expression for absorption when $N_2 << N_1$). Since the phase, frequency, and direction of the emitted photons are, within uncertainty principle limits, identical to those of the stimulating radiation, coherent addition results with amplification of the incident radiation. With suitable feedback provided by mirrors, oscillation will result, and a coherent output beam will be emitted if one of the feedback mirrors is made partially transmitting.

The arguments may be extended to multilevel systems by invoking the principle of detailed balance (but note however that inversions, or departures from thermal equilibrium, are only possible on

limited pairs of transitions). Then at thermal equilibrium the processes in figure 1 may be compared with the Planck radiation law to give $B_{12} = B_{21}$ as before, but also to show that

$$\frac{A_{21}}{B} = \frac{8\pi h^3}{c^3} \nu^3 \qquad (2)$$

independent of the oscillator strength which governs both A_{21} and B in the same way. We see from equation (2) that spontaneous emission competes more and more successfully with stimulated emission as the transition wavelength is reduced. It is for this reason that the first stimulated emissive devices (Masers) were demonstrated in the microwave region and explains why there has been a trend to shorter wavelengths with improving technology; X-ray laser operation is still problematic.

MOLECULAR SPECTROSCOPY OF CARBON DIOXIDE (Ref. 2)

Normal Modes of Vibration

A system of coupled oscillators, typified on the microscopic scale by a simple molecule, can in general carry out a very complex Lissajous motion. It may be shown that all such motions arise from the addition of excitations of 'normal modes' in the correct phase. Carbon dioxide is a linear symmetric triatomic molecule and thus possesses three normal modes, illustrated schematically in figure 2. The bending mode is doubly degenerate. The modes are named and numbered as shown and some insight into their frequencies ω_i may be obtained by assumption of a simple valence force field model. This model joins the point masses with springs which do not interact and which possess force constants k_b and k_s for bending and linear extension respectively. Preserving linear momentum and assuming simple harmonic motion leads to the relations

$$\omega_1^2 = k_s/m_o; \quad \omega_2^2 = k_b \frac{1 + \frac{2m_o}{m_c}}{m_o}; \quad \omega_3^2 = k_s \frac{1 + 2\frac{m_o}{m_c}}{m_o} \qquad (3)$$

Despite the simplistic approximation ($\omega_3/\omega_1 = 1.76$; calc. = 1.91) these relations turn out to be very useful for calculating isotopic shifts. The 'springs' have force constant k_s of about 1000 dyne/cm, like typical small man-made springs. The masses are of course very small, about 10^{-26}g. Consequently the vibration frequencies are over 10^{13} Hz.

Vibrational Energies

Solution of the Schrödinger equation for the parabolic potential of a harmonic oscillator yields eigenvalues E_i of $(v_i + d_i/2)\ \hbar\omega_i$, a ladder of equally spaced rungs. v_i is the vibrational quantum number and d_i is the degeneracy of the level. Anharmonicity causes the ascending rungs to get closer together. The energy level diagram of the low-lying vibrational states of CO_2 appears in figure 3. States are labelled as $(v_1 v_2^{\ell} v_3)$ where ℓ is the number of quanta of vibrational angular momentum in the bend. The (100) and (02^{0}0) states interact by Fermi resonance and so the resulting states are mixed and shifted in energy, but this is normally ignored in labelling transitions. Subsequently it will

be shown that it is fairly easy to selectively excite ("pump") $v_3 = 1$ to give inversions over $v_1 = 1$ or $v_2 = 2$. The resulting oscillation occurs in bands at about 9 and 10 microns wavelength. Isotopic substitution by ^{13}C and/or ^{18}O shifts the vibrational levels by amounts computable from the valence force field results with a consequent small change in oscillation frequency. There is no longer an automatic coincidence with the 626 'normal' isotopic CO_2 present in the atmosphere, with less resultant atmospheric absorption. This can be of special benefit for long-range remote-sensing systems. 'Sequence band' operation has been obtained on transitions such as (011) → (110), in which an extra bending quantum is present in both lower and upper laser levels; these are shifted to longer wavelength than the (001) → (100) transitions by anharmonic effects.

Rotational Structure

The solution of Schrödinger's equation for a rigid rotor yields a set of energy levels which are not equally spaced. To first order

$$E_J = BJ(J+1) \qquad (4)$$

where $B = \frac{h}{8\pi^2 Ic}$ and J is the rotational quantum number.

Since molecules can vibrate and rotate their total energy is to a good approximation given by the sum of the vibrational and rotational contributions. Since from the above formula rotational quanta are rather small – B is 0.39 cm^{-1} for CO_2 – the resultant energy level diagram is as shown in figure 4. Here some strong laser transitions in the molecule are included. Several features are immediately apparent. The selection rule $\Delta J = \pm 1$ is seen to govern the changes in J; the transition $J \longrightarrow J+1$ is termed the R(J) line, while $J \longrightarrow J-1$ is called P(J). Alternate levels are missing due to nuclear spin statistics: the nuclear spins of ^{16}O and ^{18}O are zero. The rotational dependence of the matrix elements governing the oscillator strength is roughly the same as the rotational degeneracy, so the distribution of gain among the rotational levels closely follows the thermal distribution, peaking at about J = 20. Because rotational relaxation and rotational – translational energy transfer is exceedingly rapid, the rotational levels tend to thermalise at the ambient gas temperature. The vibrational levels are inverted, however, and this leads to an enhanced gain on the P branch transitions. Maximum gain occurs around P(20), which dominates the output unless a dispersive element is placed within the laser cavity to select other transitions.

POPULATION INVERSION MECHANISMS (Ref. 3)

Electron Impact

Although CO_2 lasers can be pumped by a variety of means, the most important is electrical, and is the only method to be considered here. Electrons present in the 'glow discharge' type of plasma, which will be discussed in more detail later, impact molecules and in so doing lose some of their kinetic energy to excitation of the molecule. In the Born approximation for electric-dipole transitions, the cross sections for electron impact excitation are proportional to the optical cross sections, and thus it would be expected that the upper laser level could be populated by this means. On the other hand, neither of the lower states (100) and (020) would be populated; in the first case because the vibration

induces no dipole, and in the second because the selection rule $\Delta v = 1$ would be broken. Thus it should be possible to set up a population inversion by this selective excitation technique. Although the Born approximation is not expected to be accurate for electrons of such low energy as encountered in practice in glow discharges, the very first CO_2 laser to be operated did in fact depend on this pumping scheme.

Resonance Transfer

It was soon discovered that a great enhancement in laser power output and efficiency could be obtained by including nitrogen in the laser gas mixture. Energy transfer occurs from vibrationally excited nitrogen ($v = 1$) to the CO_2 ($v_3 = 1$) level at a very high rate, 1.9×10^4 $torr^{-1}sec^{-1}$, because of the extremely close coincidence in energy of these two states; the energy difference is only 18 cm^{-1}. The $v = 1$ level of nitrogen has a very long radiative lifetime since there is no dipole, and the cross-section for electron impact excitation, shown in fig. 5, extends over a broad electron energy range due, not to the forbidden dipole process, but to the existence of an unstable N_2^- state. $N_2(v = 1)$ is thus a near-ideal energy transfer agent.

Relaxation Processes

The optical inactivity of the transition from ground state to lower laser levels has already been mentioned. Thus the radiative lifetimes of these levels is very long, and some other process must be found to empty these levels during laser action, otherwise the population inversion cannot be maintained. Collisional relaxation is the key process; for instance, there is only a 50 cm^{-1} energy mismatch in the processes

$$CO_2(100,\ 02^{\circ}0) + CO_2\ (000) \rightarrow 2CO_2\ (010) \qquad (5)$$

However it remains to find a rapid means of collisionally removing $CO_2(010)$ or even better the lower laser levels directly. At the same time collisional relaxation of the upper laser level, $CO_2(001)$, is highly undesirable since it competes with the pumping process. Fortunately it is found that helium fulfills these criteria admirably, and at the same time is chemically inert and provides an excellent 'buffer gas' in which to run the electric discharge.

Hence, CO_2 lasers are almost invariably operated in a gas mixture containing helium and nitrogen as well as carbon dioxide; the former relaxes the lower laser level and the latter pumps the upper laser level by resonant energy transfer.

PULSED GLOW DISCHARGES (Ref. 4)

Introduction

Numerous definitions of plasma exist; none are entirely satisfactory. For our purposes the following will suffice: an ionised gas maintained in a steady state by an electric field driving a current through it to balance the energy losses. The reader is probably familiar with several types of plasmas such as arcs and glow discharges. Certain properties of the plasma required have already emerged

from previous sections. The gas temperature must be kept fairly low to avoid thermal population of the lower laser level; the exact value depends on a number of parameters such as pumping rate but certainly 100°C should be looked on as rather high. On the other hand, the electron energy required to excite the vibrational states of nitrogen is 2–3 electron volts (see fig.5), which corresponds to an electron temperature of order 30,000K. In fact the enormous mass ratio between electrons and molecules leads to restricted energy exchange and it is indeed possible to produce a plasma which departs from thermal equilibrium with an electron temperature of about 1eV and a gas temperature around ambient; it belongs to a class known as glow discharges. The gas mixture must contain CO_2 and nitrogen in roughly equal amounts, generally with an excess of helium. It has been experimentally established that extraction of reasonable energy from a fairly compact device requires quite a high molecular density, approaching or roughly equal to one atmosphere.

Steady-State Operation

A number of processes operate which ultimately lead to the mutual neutralisation of the separated charges in a plasma, and the plasma can only exist in a steady state if the rate of production of ions and free electrons balances these loss processes. The carbon dioxide laser can be operated using continuously working or pulsed discharges; while all of the foregoing sections apply equally well to both types, the discharge stability conditions are quite different and lead to quite different engineering designs. In cw lasers, the loss process is predominantly ambipolar diffusion to the wall; in pulsed devices there is insufficient time for this to happen and the plasma adjusts to a condition where gas-phase recombination or electron attachment to neutral species dominate losses. We will now investigate how the rates of these processes can be quantified in order to gain some insight into the conditions within the plasma.

The ionisation rate by impact of plasma electrons may be obtained as follows. For a monoenergetic stream of electrons of velocity v_e and density n_e passing through a gas of molecular density N_o and ionisation cross section per molecule $Q_i(v)$, simple kinetic theory gives an ionization rate per unit volume $Z_i(v)$ of

$$Z_i(v) = n_e N_o v_e Q_i(v) \tag{6}$$

Generalising to electrons distributed in energy such that $f(\epsilon)d\epsilon$ is the fraction of n_e in the range ϵ to $\epsilon + d\epsilon$, we find

$$dZ_i = N_o v_e Q_i dn_e \tag{7}$$

$$v_e \rightarrow \left[\frac{2\epsilon}{m}\right]^{\frac{1}{2}}, \qquad dn_e \rightarrow n_e f(\epsilon)d\epsilon$$

so that

$$Z_e = n_e N_o \int_{\epsilon_i}^{\infty} \left[\frac{2\epsilon}{m}\right]^{\frac{1}{2}} Q_i(\epsilon) f(\epsilon) d\epsilon \tag{8}$$

or $$Z_i = n_e N_o S_i \tag{9}$$

where ϵ_i is the ionisation threshold energy.

If further the electron distribution is Maxwellian with a temperature T_e, then

$$f(\epsilon) = 2\left[\frac{\epsilon}{\pi}\right]^{\frac{1}{2}}\left[kT_e\right]^{-3/2}\exp - \left[\epsilon/kT_e\right] \qquad (10)$$

Figure 6 shows a typical shape of an ionisation cross-section and Maxwellian electron energy distribution. We are concerned with the integral of the product of $Q_i(\epsilon)$ and $f(\epsilon)$, and it is clear from the diagram that under normal circumstances only the high energy tail of the distribution overlaps the cross-section above threshold. Thus the Maxwellian provides the high energy cutoff to the integral, which is not very sensitive to the shape of the ionisation cross-section $Q_i(\epsilon)$. The latter may be approximated by any sensible function such as a step or linear ramp and it is always found that

$$S_i = \left[\frac{8}{\pi m}\right]^{\frac{1}{2}} Q_i(\max)\,\epsilon_i^{\frac{1}{2}}\,\varphi\left[\frac{\epsilon_i}{kT_e}\right]\exp - \left[\epsilon_i/kT_e\right] \qquad (11)$$

where φ is a very slowly varying function of T_e of order unity. Clearly ionisation of the species having the lowest IP is strongly favoured in mixtures of gases and in the CO_2 laser mixture the dominant ionisation will be of CO_2 itself. Of course just as many electrons will be formed as positive ions in the process

$$e + CO_2 \rightarrow CO_2^+ + 2e \qquad (12)$$

so the ionisation rate is identical to the electron production rate. However, a series of complex ion-molecule reactions ensure that CO_2^+ is by no means necessarily the dominant positive ion in the plasma. Equation 11 reveals that the ionisation rate rises dramatically with electron temperature, and this is shown schematically in figure 7. Here typical attachment and recombination plots for CO_2 laser gas mixtures are included. The attachment process

$$e + M \rightarrow M^- \qquad (13)$$

suffers from the usual conservation restrictions, and processes such as dissociative attachment which are not so impeded tend to predominate; e.g

$$e + CO_2 \rightarrow CO + O^- \qquad (14)$$

These attachment processes have a threshold at lower energy than ionisation, so their T_e dependence is as shown in figure 7. Electron-ion recombination coefficients actually fall slowly with T_e because recombination is facilitated by the smaller the relative velocity and hence the longer the 'contact time' between electron and ion. On the other hand the negative ion produced by electron attachment can rapidly recombine with positive ions and be removed.

Self-Sustained Operation

With these arguments and by referring to figure 7 we are in a position to understand the determinants of electron temperature in real devices. Provided that some 'preionisation' (to be discussed later) is present, the discharge will settle down after application of sufficient voltage to run at point a, where ionisation balances attachment. Certain substances such as hydrogen cause electron 'detachment' from negative ions thus reducing the apparent attachment coefficient and operating electron temperature. Under conditions of strong detachment the loss processes become dominated by recombination and the self-sustained discharge operates at point c. Since $kT_e \approx$ energy gained by electron/mean free path = $eE\lambda$, where E is the electric field present in the plasma and the m.f.p $\lambda \propto N_o^{-1}$, we see that there must be a one-to-one correspondence between T_e and E/N_o, the so-called 'reduced' electric field. Consequently, the field at which the discharge runs is not freely variable in the self-sustained regime, but is set by the electron temperature at which ionisation balances attachment or recombination. In typical CO_2 laser mixtures, E/N assumes a value of 10-15 kV/cm atmosphere (3.7 - 5.6 x 10^{-16}Vcm^2). Note that the actual steady-state value of n_e, and thus discharge current, has not entered the discussion, and indeed the current is here determined only by external circuit restraints and can be varied widely at fixed voltage; values of order 200A/cm^2 are not unusual in self-sustained devices.

Electron-Beam-Sustained Operation

Calculations of the type described for ionisation by electron impact are trivially extendable to other impact processes. If instead of the ionisation cross-section we use the vibrational excitation cross-section for nitrogen shown in figure 5, we obtain the excitation rate essentially of the upper laser level. Varying the electron temperature reveals that this process occurs with maximum efficiency at a reduced field of near 4kV/cm atm (1.5 x 10^{-16}Vcm^2), much lower than typical self-sustained laser operating points. If we could ionise the gas by some means other than electron impact by plasma electrons of energy $\sim kT_e$, it may be possible to choose the reduced field, and thus operate at a more optimal value. This can indeed be done by firing high energy electrons (E $\approx$ 100 keV) through a thin foil 'window' into the gas which is ionised by impact with these externally supplied projectiles. The electron temperature may then be set by appropriate choice of an applied electric field which drifts the 'secondary' electrons and positive ions produced by the high-energy electrons towards the electrodes. If the electron temperature is set below T_c in figure 7, it is seen that recombination is the dominant loss process. In the absence of detaching species, attachment dominates losses from T_c to approaching T_a, the point near which self-sustained operation takes over. As detaching species are added recombination dominates the loss processes for increasing T_e.

The steady-state operating current in externally-sustained discharges is not set by the external circuit. For a primary electron transmitted at a current density of J_p, the ionisation and secondary electron production rate is

$$\frac{dn_e}{dt} = J_p \frac{\sigma}{e} N_o \qquad (15)$$

where σ is the collisional ionisation cross-section by high energy electrons. In the attachment-dominated regime, the loss rate is

$$-\frac{dn_e}{dt} = \beta N_o n_e \qquad (16)$$

where β is the attachment coefficient. Thus the equilibrium secondary electron density is

$$n_e = \frac{J_p \sigma}{e\beta} \tag{17}$$

and consequently the secondary current density J_s amounts to

$$J_s = n_e e\bar{v} = \frac{J_p \sigma}{\beta} \bar{v} \tag{18}$$

where $\bar{v}$ is the drift velocity under the action of the applied field. We see that the secondary current can be substantially greater than the primary, and the 'magnification ratio' M is

$$M = \frac{J_s}{J_p} = \frac{\sigma}{\beta} \bar{v} \tag{19}$$

M is typically of order one thousand. The discharge in this regime is ohmic, with an impedance Z of

$$Z = \frac{Ed}{J_s A} = \frac{d}{A} \left[\frac{\beta}{J_p \sigma \mu} \right] \tag{20}$$

where d and A are the discharge gap and area, respectively, and μ is the electron mobility $\bar{v}/E$. The discharge has conductivity $(J_p \sigma \mu/\beta)$, and its impedance is normally of order 10 ohms.

Stability Conditions

Self-sustained discharges are inherently unstable. Suppose a region of increased electron density forms near one electrode. This will have an enhanced conductivity relative to the rest of the plasma and will tend to 'short-out' some of the field in the gap. Consequently the field in the remainder of the gap will be increased and so too will the ionization rate, which will exceed the loss rate and lead to an uncontrolled growth of n_e-- an 'avalanche'. Thus the region of increased n_e grows until the gap is bridged by a highly conducting streamer--an arc. Since the arc column is so highly conducting it can sustain current densities many orders greater than glow discharges and so is normally constricted in cross-section. Once established, the conductivity is so high that the electric field, and thus electron temperature, are rather low, insufficient for electron-impact ionisation to exceed losses. On the other hand n_e is so high that collisions with neutral species are so frequent that thermalisation occurs, with the gas temperature being greatly raised above ambient. Under these circumstances the ionisation is maintained thermally ('Saha process').

Arcs are quite unsuitable for pumping carbon dioxide lasers due to the approximate equality of their gas and electron temperatures; true thermal equilibrium is reached so a vibrational inversion cannot be produced. The glow-to-arc transition described above is therefore highly undesirable, and several techniques are used to avoid it. Firstly, the arc takes a small but finite time to develop ($\sim$ 1 μs), so that it can be avoided if steps are taken to ensure that the glow discharge is of short duration; low inductance and resistance capacitor-discharge circuits are required. Secondly, the electrode surfaces

must be as smooth as possible to avoid local field enhancements due to surface irregularities. Thirdly, it is necessary to 'preionise' the gas before application of the electric field with about 10^7 electron cm^{-3} to avoid the effects of statistical fluctuations on the initial starting avalanche processes. This is generally ensured by UV or X-ray photoionisation of the gas in the gap, or by photoelectric emission from the electrodes. Conversely, species which readily attach electrons increase the likelihood of the glow-to-arc transition and should be avoided. Oxygen is a good example with an upper limit for stable operation of less than 1%, and since it is produced by dissociation of the carbon dioxide, this process needs to be minimised; it will be discussed at more length in the section on plasma chemistry.

Electron-beam sustained discharges are very stable. Fluctuations in n_e do not alter the ionization rate since this depends on the injected flux of primary electrons; ionisation by secondary electron impact is negligible since the electron temperature is chosen, by the appropriate impressed field, to be low, and optimal for pumping N_2 (v = 1). Consequently these discharges are much more tolerant of attaching species such as oxygen, and the limit is set by considerations of impedance mismatch of discharge to pulse forming network or even of carbon dioxide loss. A typical value of several percents of oxygen can be tolerated with graceful performance fall-off rather than catastrophic arcing.

REPRESENTATIVE DEVICES

With the scientific principles discussed, it is possible to examine engineering designs of pulsed CO_2 lasers. Of course very large numbers of designs have evolved for specific applications; here we consider a typical 'single shot' mini-TEA (transversely-excited atmospheric pressure configuration) laser and an electron-beam sustained device, and then examine the consequences of operation at significant repetition rates.

Mini-TEA Laser

Because operating fields increase with pressure, at one atmosphere the field in a self-sustained laser is measured in tens of kilovolts per centimetre. In order to keep operating voltages at reasonable levels, the discharge length along the field direction must be very short. This led to the development of the transversely-excited atmospheric pressure configuration (TEA) with the field orthogonal to the optical axis. A good example is the miniature TEA laser shown in figure 8, of the kind used for tactical rangefinding. A typical discharge section is 1 x 1 x 10 cm and output energy 100 mJ. Profiled electrodes ensure that the field nowhere exceeds that in the discharge. Preionisation is produced here by a row of UV - emitting arcs running parallel to the profiled electrodes. A CO oxidation catalyst to maintain gas life is placed somewhere within the structure which is filled to 1 atmosphere with the typical laser mixture, and the field is applied from a low inductance capacitor through a triggered spark-gap switch (not shown). The resulting current pulse lasts only a few hundred nanoseconds, insufficient time for the glow-arc transition to take place. The optical output consists of a short spike of duration about 50ns in which most of the population inversion is destroyed, followed by a 'tail' of duration about 1μs in which energy continues to transfer gradually from vibrationally excited nitrogen. The energy loading of the discharge is limited to a few hundred Joules per litre by thermal population of the lower laser level. The high operating electron temperature gives a multimode efficiency of somewhat less than 10%, and a single mode efficiency rather lower still. Such a device offers very simple construction, and can be operated at up to a few pulses per second without gas flow, when convection and thermal diffusion occur fast enough to adequately cool the laser gas mixture.

Electron-Beam Sustained Laser

Figure 9 shows the cross-section through an electron-beam sustained device. This can be operated at the optimum 4kV/cm atmosphere and give multimode efficiencies in excess of 20%. The construction is much more complex than self-sustained devices, however, and lends itself best to large volume discharges which can operate stably in this mode. An electron gun is needed to produce the high energy primary beam. This may operate by field emission, thermionic emission, or ion bombardment, and at least some designs can run for tens of microseconds. Thus the facility exists for 'long pulse' operation of the laser, with roughly rectangular output pulses of duration several microseconds or more. The high voltage pulse to the gun is often produced using a pulse transformer and pulse-forming network. Since the gun is a vacuum or very low pressure device the foil separating it from the main discharge (at about an atmosphere) must be well supported. Many of the electrons are stopped by the foil (transmission about 70%) so at appreciable repetition rates the foil support structure must be cooled. Finish and profile of the electrodes are much less critical than for self-sustained devices since the applied field is such that avalanching is insignificant.

Repetition-Rate Operation

Above a pulse repetition frequency (prf) of a few Hz, diffusion and convection are inadequate to cool the gas, which will become hotter with each successive pulse and laser action will cease. Fluctuations in gas density will cause fluctuation in E/N, and thus also lead to discharge instability. It is necessary to deliberately force gas around the system in a flow loop to renew the mixture between pulses. Figure 10 shows a schematic cross-section through such a device. The flow is usually transverse; ie. flow direction, optical axis, and electric field are all orthogonal. The ductwork incorporates a heat exchanger to maintain the gas at the required temperature and a catalyst artifact to oxidise CO to CO_2. The latter is normally fitted close to the discharge on the downstream side to enhance the catalytic activity by use of the unwanted gas heating. Some kind of fan or impeller is built into the ductwork to circulate the gas at the required rate, and to expedite this process it is important, especially at high prf, to minimise the flow impedance of the heat exchanger and catalyst.

PLASMA CHEMISTRY (Ref. 5)

Introduction

We have already seen that carbon dioxide lasers are normally filled with a mixture of nitrogen, carbon dioxide, and helium. In addition it is often difficult to entirely eliminate water vapour from the laser envelope since it is difficult to completely clean many constructional materials. Although these appear a rather unpromising set of reactants, they are subjected in the plasma to a number of energetic processes such as electron impact which can excite and dissociate molecules. Further neutral and ion-molecular reactions then ensue to give rise to interesting and important chemical effects. Obviously the loss of carbon dioxide by dissociation to carbon monoxide and oxygen is directly relevant, but the subsequent oxidation of oxygen and nitrogen to ozone and NO_x can give rise to an oxygen deficit for any catalysis of the CO/O_2 recombination reaction. These and other processes will be explored next.

Carbon Dioxide Dissociation

There are known to be two channels for the dissociation of carbon dioxide by electron impact:

$$e + CO_2 \rightarrow CO + O + e \quad (21a)$$

$$e + CO_2 \rightarrow CO + O^- \quad (21b)$$

The former (21b) has a much larger cross-section but higher threshold than the dissociative attachment process (21b), as shown in figure 11. The dissociation rate for any particular electron temperature may be found using the formalism of equation 11. For self-sustained discharges reasonable agreement is found between the measured dissociation rate, of order 10^{21} molecules/coulomb passed (dependent on gas composition, device size, etc), and calculation assuming the process occurs in the bulk of the gas. In this case the relatively high value of T_e leads to the process (21a) being dominant. Electron-beam sustained discharges are normally operated at a much lower electron temperature and the exponential in equation 11 gives rise to very low calculated values of the bulk dissociation by either process. Experimental measurements reported elsewhere in these proceedings, while much lower than comparable self-sustained devices, are higher than the bulk calculations. The same experiments indicate that the dissociation is occurring in the high T_e region of the sheath associated with electron emission from the cathode.

Knowledge of the dissociation rates, coupled with tolerance to dissociation products - namely oxygen, since carbon monoxide does not attach - allows specification of the CO oxidation catalyst. However there are other reactions which can occur with which the catalyst may have to deal.

Oxygen Loss

In experiments on both self-sustained and e-beam sustained CO_2 lasers, it has been observed that, at least initially, carbon monoxide and oxygen are not formed in their correct stoichiometric ratio of 2:1, but in a ratio greater than 2.0. This implies that oxygen is being lost to form other compounds and is therefore unavailable for CO oxidation (although significant CO_2 loss has not been observed in small TEA lasers up to 2×10^7 pulses). These processes therefore merit closer examination, although at the time of writing limited experimental or theoretical progress has been made, largely due to the complexities of the possible reactions. Once carbon dioxide dissociation has taken place, two new species have been added to the gas, one of which, atomic oxygen, is particularly reactive. The reverse reaction

$$O + CO\ (+M) \rightarrow CO_2(+M) \quad (22)$$

is spin forbidden and proceeds at a negligible rate. The rate constant for the three-body association of oxygen atoms is high, reflecting the spin conservation of the process

$$O + O\ (+M) \rightarrow O_2\ (+M) \quad (23)$$

Once molecular oxygen has been formed, it can undergo further reaction with atomic oxygen to form ozone

$$O + O_2 \ (+M) \rightarrow O_3 \ (+M) \qquad (24)$$

by a fast allowed process. Reaction of oxygen atoms with nitrogen to give nitrous oxide is spin forbidden and to give nitric oxide and nitrogen atoms is highly endothermic; oxygen atoms do not react with nitrogen. Nitrogen oxides are probably formed by several routes. The associative detachment reaction

$$O^- + N_2 \rightarrow N_2O + e \qquad (25)$$

can produce nitrous oxide from the small amounts of O^- present in the plasma; the product is probably immune to further oxidation. Nitrogen atoms formed by dissociative electron–ion recombination of N_2^+ undergo reactions of the kind

$$N + O + M \rightarrow NO + M \qquad (26)$$

followed by

$$NO + O + M \rightarrow NO_2 + M \qquad (27)$$

However once some ozone and nitrogen oxides are formed they are subject to destruction by such processes as

$$NO + O_3 \rightarrow NO_2 + O_2 \qquad (28)$$

$$O + NO_2 \rightarrow NO + O_2 \qquad (29)$$

so they do not reach high concentrations. Undoubtedly the complete reaction set is much more complex, with three–body ion–molecule reactions probably playing an important part; unfortunately the rate constants of the latter are not well known, only four being included out of 167 possible reactions in one computer simulation! Nevertheless it would be useful to catalyse exothermic destruction reactions such as

$$2NO + 2CO \rightarrow N_2 + 2CO_2 \qquad (30)$$

and $$N_2O + CO \rightarrow N_2 + CO_2 \qquad (31)$$

Designers of CO oxidation catalysts need therefore to allow for oxidation not just by oxygen, but also the oxides of nitrogen and ozone.

While the direct association of CO and oxygen atoms takes place at a negligible rate, the reaction

$$OH + CO \rightarrow CO_2 + H \qquad (32)$$

goes very quickly. Hydroxyl radicals can be formed readily from oxygen atoms in the presence of water vapour by the process

$$O + H_2O \rightarrow 2OH \qquad (33)$$

while the dissociative attachment and ionisation reactions

$$e + H_2O \rightarrow OH + H^- \qquad (34)$$

$$e + H_2O \rightarrow OH + H^+ + 2e \qquad (35)$$

also yield hydroxyl. Thus, carbon monoxide readily reacts with oxygen in the presence of water vapour via reaction (32); the hydrogen atoms complete the chain via

$$H + O_2 \rightarrow OH + O \qquad (36)$$

to regenerate hydroxyl, with the net reaction

$$CO + O_2 \rightarrow CO_2 + O \qquad (37)$$

There is a plethora of further radical and atom loss processes analogous to those described in the previous section, but the overall conclusion is that water vapour behaves as a very effective homogeneous catalyst for carbon monoxide oxidation. It is to be expected that the plasma is the initial source of hydroxyl radicals, both directly from processes (34) and (35) and via the formation of oxygen atoms followed by (33). Thus the effectiveness of water vapour (or hydrogen, which readily reaches equilibrium with water in the plasma) as a catalyst should depend on the plasma electron temperature. Limited experimental work has been undertaken on homogeneous catalysis in CO_2 lasers, but it appears that hydrogen and CO are effective discharge stabilisers in helium–rich mixtures but not in mixtures containing little or no helium. This could be due to the difference in electron temperature, but it must also be pointed out that these molecules are effective electron detachers from negative ions, and thus tend to stabilise the discharge by this means also.

REFERENCES

1 Eyring, H., Walter, J., and Kimball, G. E.: Quantum Chemistry (Wiley, 1967), Chapter 8.

2 Herzberg, G.: Molecular Spectra and Molecular Structure II Infrared and Raman Spectra of Polyatomic Molecules (Van Nostrand, 1945).

3 Cheo, P. K.: 'CO_2 lasers' in Levine, A. K., and DeMaria, A. J.: Lasers Volume 3 (Dekker, 1971).

4 Webb, C. E.: 'The fundamental discharge physics of atomic gas lasers' and
Judd, O. D.: 'Fundamental kinetic processes in the CO_2 laser'; both in Pike, E. R.: High power gas lasers, 1975 (Inst. Phys. Conf., Ser. No 29, 1976).

5 Von Engel, A.: Electric plasmas, their nature and uses (Taylor & Francis, 1983), Chapter 10.
Smith, I. W. M.: 'Reactive and Inelastic Collisions involving molecules' in Gas Kinetics and Energy Transfer, Vol 2. (The Chemical Society, 1977).
Hokazono, H. and Fujimoto, H.: Theoretical analysis of the CO_2 molecule decomposition and contaminants yield in a TEA CO_2 laser discharge, J. Appl. Phys. 62 (5), 1585 (September 1987).

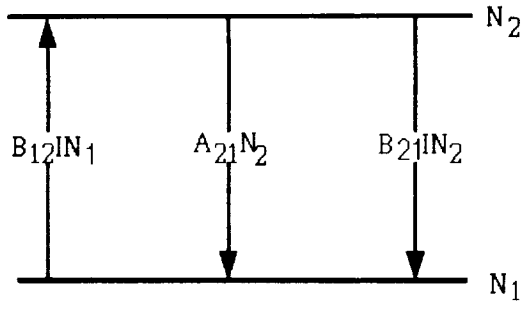

Figure 1. Radiative processes in a two-level system.

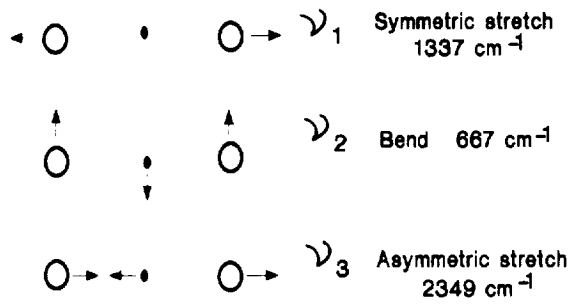

Figure 2. Normal modes of the CO_2 molecule. Frequencies are for the 626 isotope.

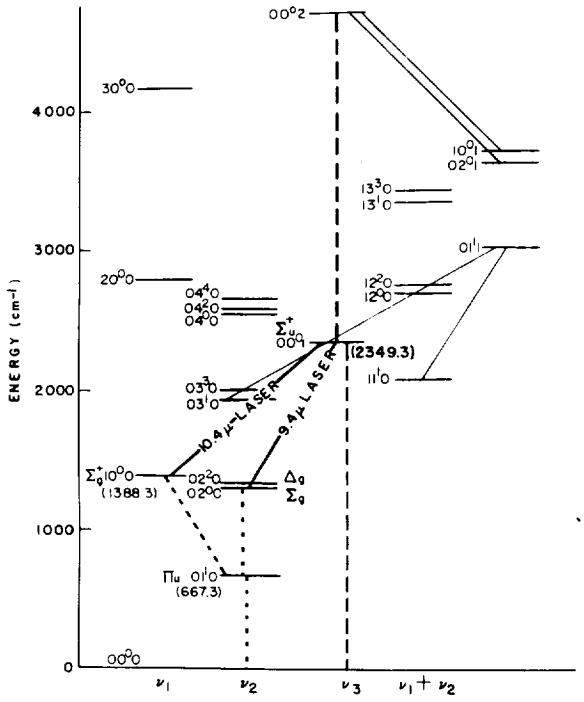

Figure 3. Energy level diagram of low-lying vibrational levels of the carbon dioxide molecule.

Permission to reproduce figure granted by American Physical Society/American Institute of Physics (Physical Review, vol. 125, p. 229, 1962).

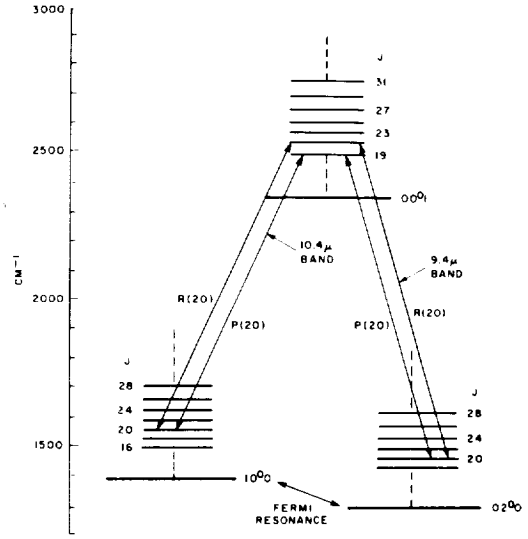

Figure 4. Total effective cross section for vibrational excitation of N_2 (V = 1 - 8) by electron impact. (After Schulz)

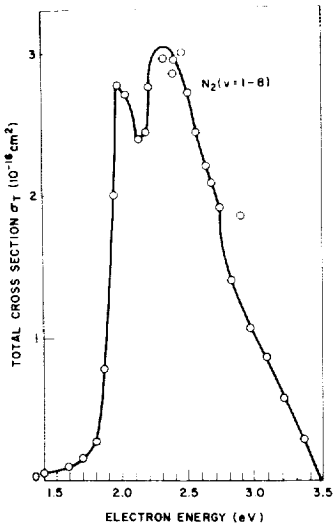

Figure 5. A detailed laser transition diagram for the 00^01 - 10^00 and 00^01 - 02^00 bands, including rotational levels.

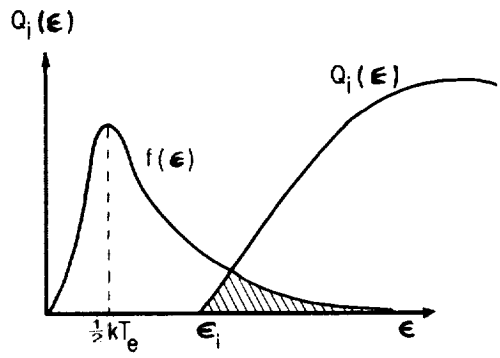

Figure 6. Ionisation cross section and Maxwellian energy distribution.

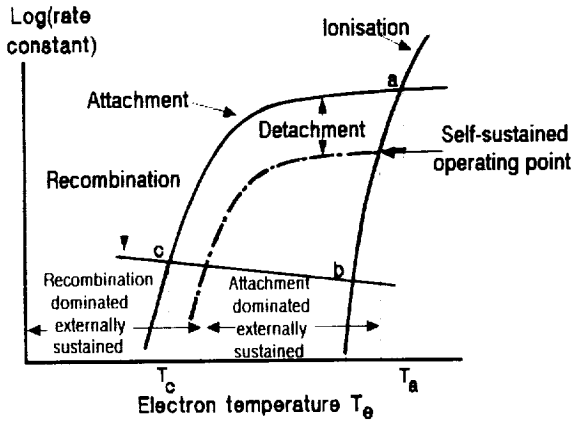

Figure 7. Ionisation and loss processes in pulsed-CO_2 laser discharges.

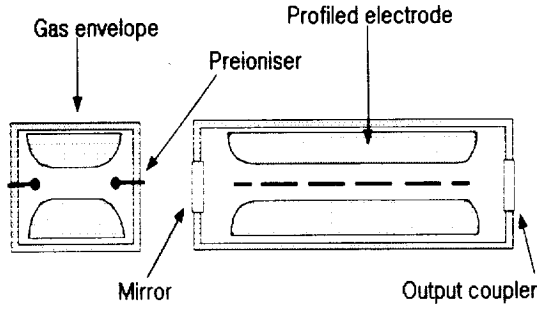

Figure 8. Schematic section through mini-TEA laser.

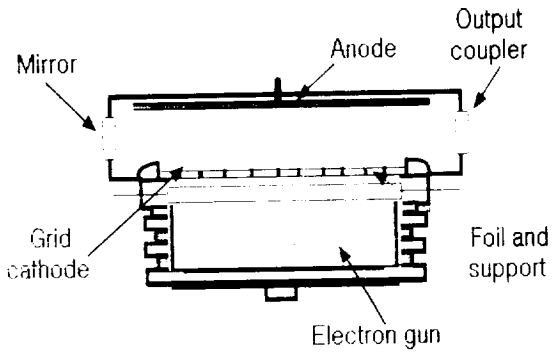

Figure 9. Schematic section through e-beam-sustained carbon dioxide laser.

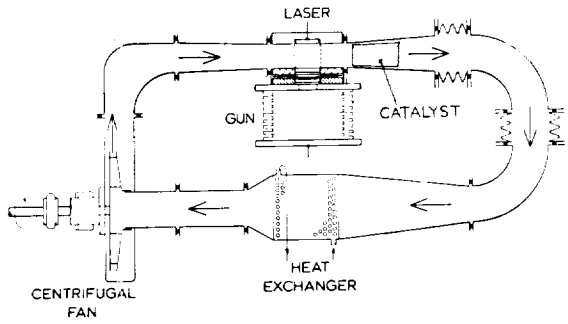

Figure 10. Schematic diagram of a high repetition rate pulsed-CO_2 laser.

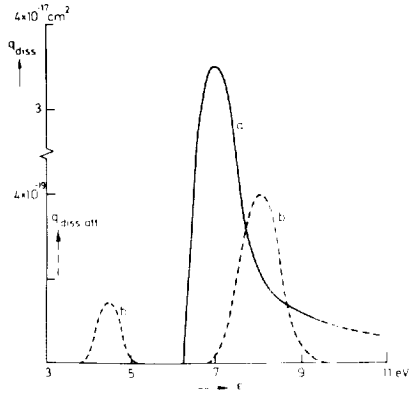

Figure 11. Dissociation $q_{diss} \cdot f(\epsilon)$ (curve a) and dissociative attachment $q_{diss\ att} \cdot f(\epsilon)$ (curves b) of CO_2.